Science Advances
AAAS

Supplementary Materials for

Tumor collection/processing under physioxia uncovers highly relevant signaling networks and drug sensitivity

Brijesh Kumar, Adedeji K. Adebayo, Mayuri Prasad, Maegan L. Capitano, Ruizhong Wang, Poornima Bhat-Nakshatri, Manjushree Anjanappa, Edward Simpson, Duojiao Chen, Yunlong Liu, Jeanne M. Schilder, Austyn B. Colter, Callista Maguire, Constance J. Temm, George Sandusky, Emma H. Doud, Aruna B. Wijeratne, Amber L. Mosley, Hal E. Broxmeyer*, Harikrishna Nakshatri*

*Corresponding author. Email: hbroxmey@iupui.edu (H.E.B.); hnakshat@iupui.edu (H.N.)

Published 12 January 2022, *Sci. Adv.* **8**, eabh3375 (2022)
DOI: 10.1126/sciadv.abh3375

The PDF file includes:

Other Supplementary Material for this manuscript includes the following:

Supplementary Tables

Table S1: Global proteomic analysis of EpCAM$^+$ tumor cells from PyMT and Her2/Neu mice collected and processed under physioxia and ambient air.

Table S2: Phospho-proteomic analysis of EpCAM$^+$ tumor cells from PyMT mice collected and processed under physioxia and ambient air.

Table S3: RNA-seq analysis of cells from ascites fluids of three patients. Genes differentially expressed under physioxia compared to ambient air are listed.

Table S4: List of genes alternatively spliced along with splicing type and location under physioxia compared to ambient air.

Supplementary Figures

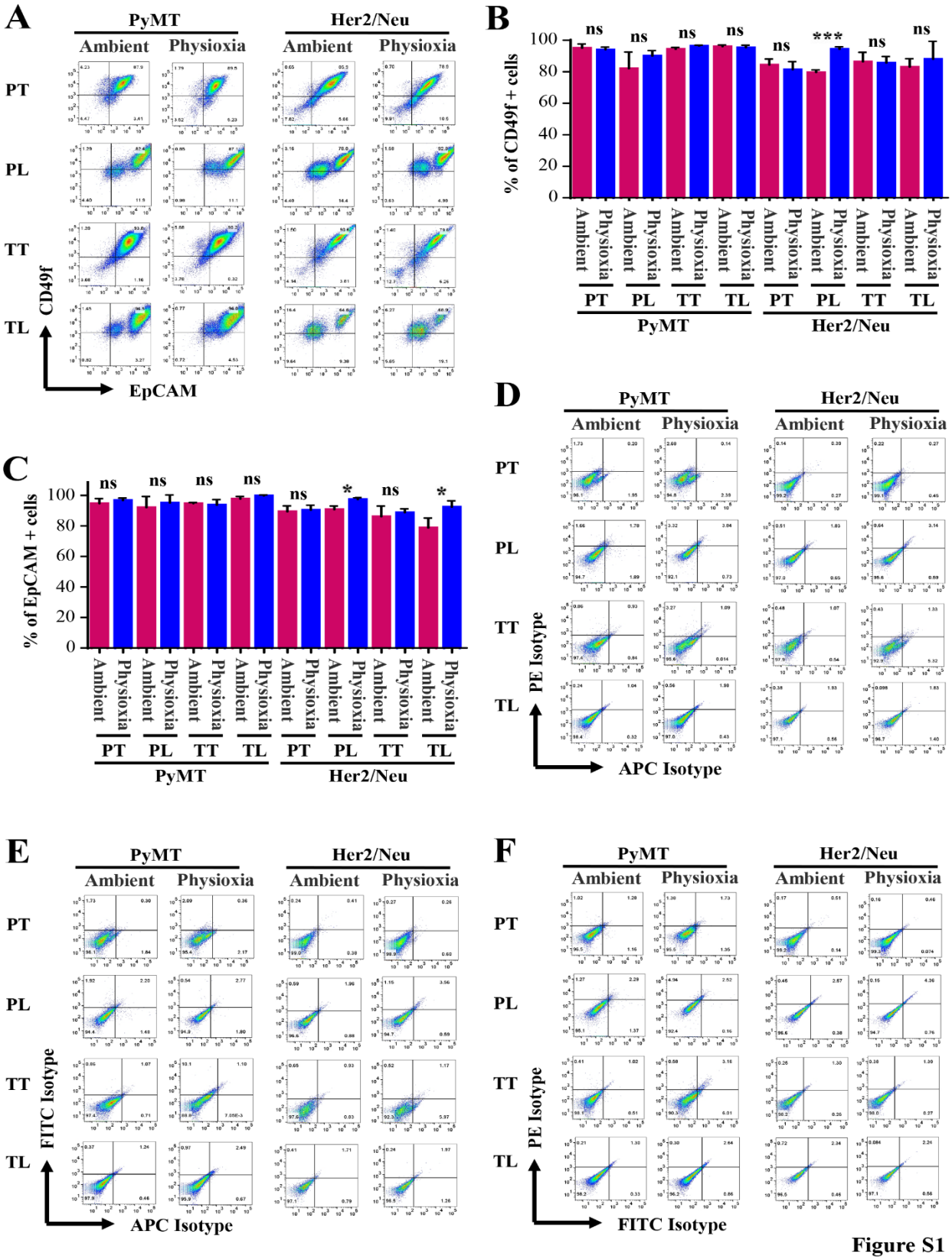

Figure S1

fig. S1: Physioxia minimally effected CD49f/EpCAM staining patterns. (A) CD49f/EpCAM staining patterns of tumor cells under physioxia and ambient air (n=3-6, one-way ANOVA). (B) Number of $CD49f^{+}$ cells were similar under two conditions except in cultured Her2/Neu tumor cells (PL). (C) Number of $EpCAM^{+}$ cells were similar under two conditions except in cultured Her2/Neu cells. (D-F) Staining patterns of isotype controls for the experiments that measured LGR5-PE/TSPAN8-APC, CD61-FITC/TSPAN8-APC, CD49f-PE/EpCAM-APC, CD274-PE/EpCAM-APC and CD24-APC/CD29-FITC. *$p<0.05$, ***$p<0.001$ by ANOVA. ns is not significant.

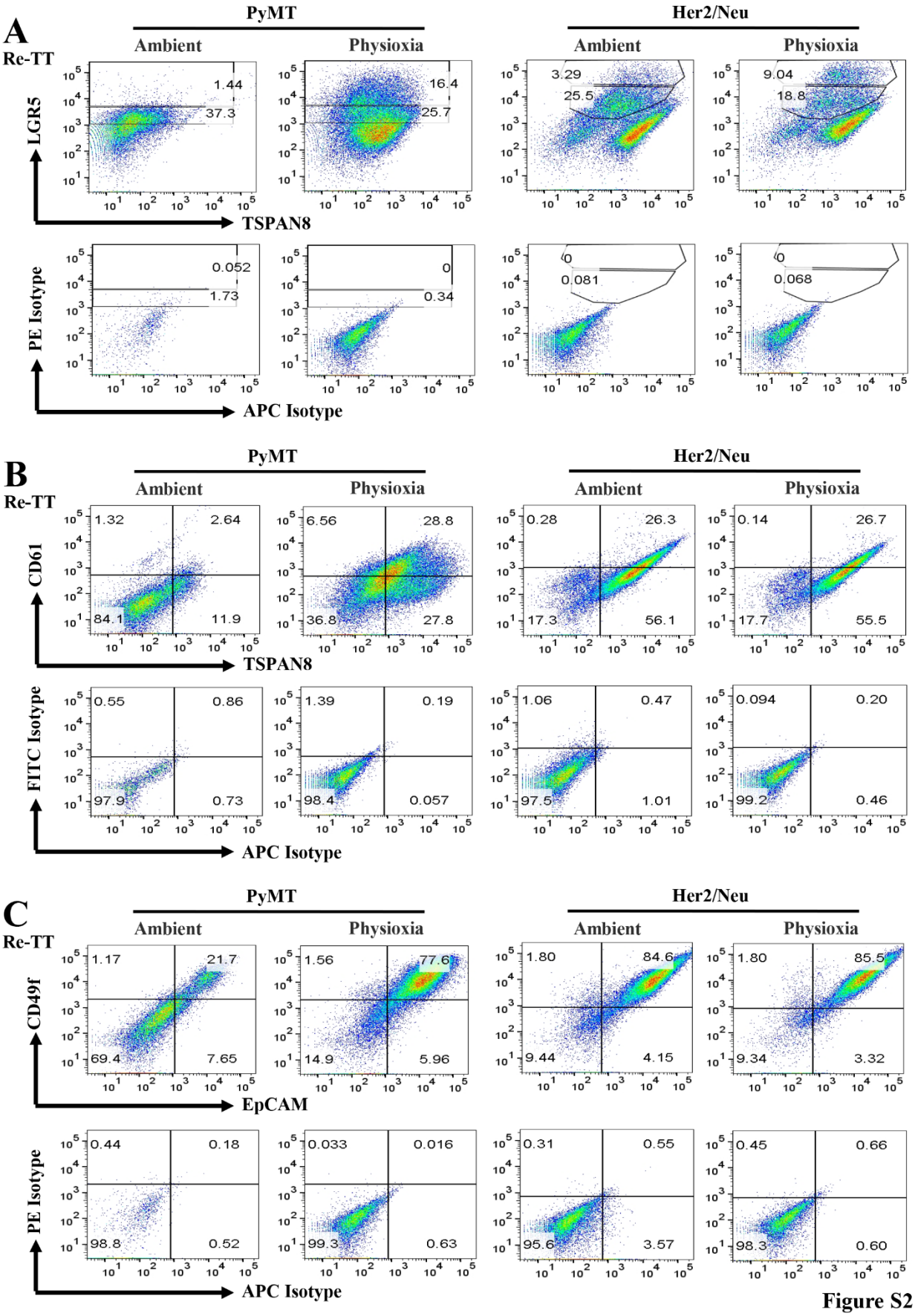
A
Re-TT
PyMT
Her2/Neu
Ambient
Physioxia
Ambient
Physioxia
LGR5
TSPAN8
1.44
37.3
16.4
25.7
3.29
25.5
9.04
18.8
PE Isotype
APC Isotype
0.052
1.73
0
0.34
0
0.081
0
0.068
B
Re-TT
PyMT
Her2/Neu
Ambient
Physioxia
Ambient
Physioxia
CD61
TSPAN8
1.32
2.64
84.1
11.9
6.56
28.8
36.8
27.8
0.28
26.3
17.3
56.1
0.14
26.7
17.7
55.5
FITC Isotype
APC Isotype
0.55
0.86
97.9
0.73
1.39
0.19
98.4
0.057
1.06
0.47
97.5
1.01
0.094
0.20
99.2
0.46
C
Re-TT
PyMT
Her2/Neu
Ambient
Physioxia
Ambient
Physioxia
CD49f
EpCAM
1.17
21.7
69.4
7.65
1.56
77.6
14.9
5.96
1.80
84.6
9.44
4.15
1.80
85.5
9.34
3.32
PE Isotype
APC Isotype
0.44
0.18
98.8
0.52
0.033
0.016
99.3
0.63
0.31
0.55
95.6
3.57
0.45
0.66
98.3
0.60

Figure S2

fig. S2: Analysis of tumors developed upon re-transplantation of cells derived from stage 3 tumors. (A) LGR5/TSPAN8 staining patterns of cells from tumors derived from stage 3 as described in Fig. 1A. (B) CD61/TSPAN8 staining patterns. (C) CD49f/EpCAM staining patterns. Representative staining patterns with isotype control antibodies are shown.

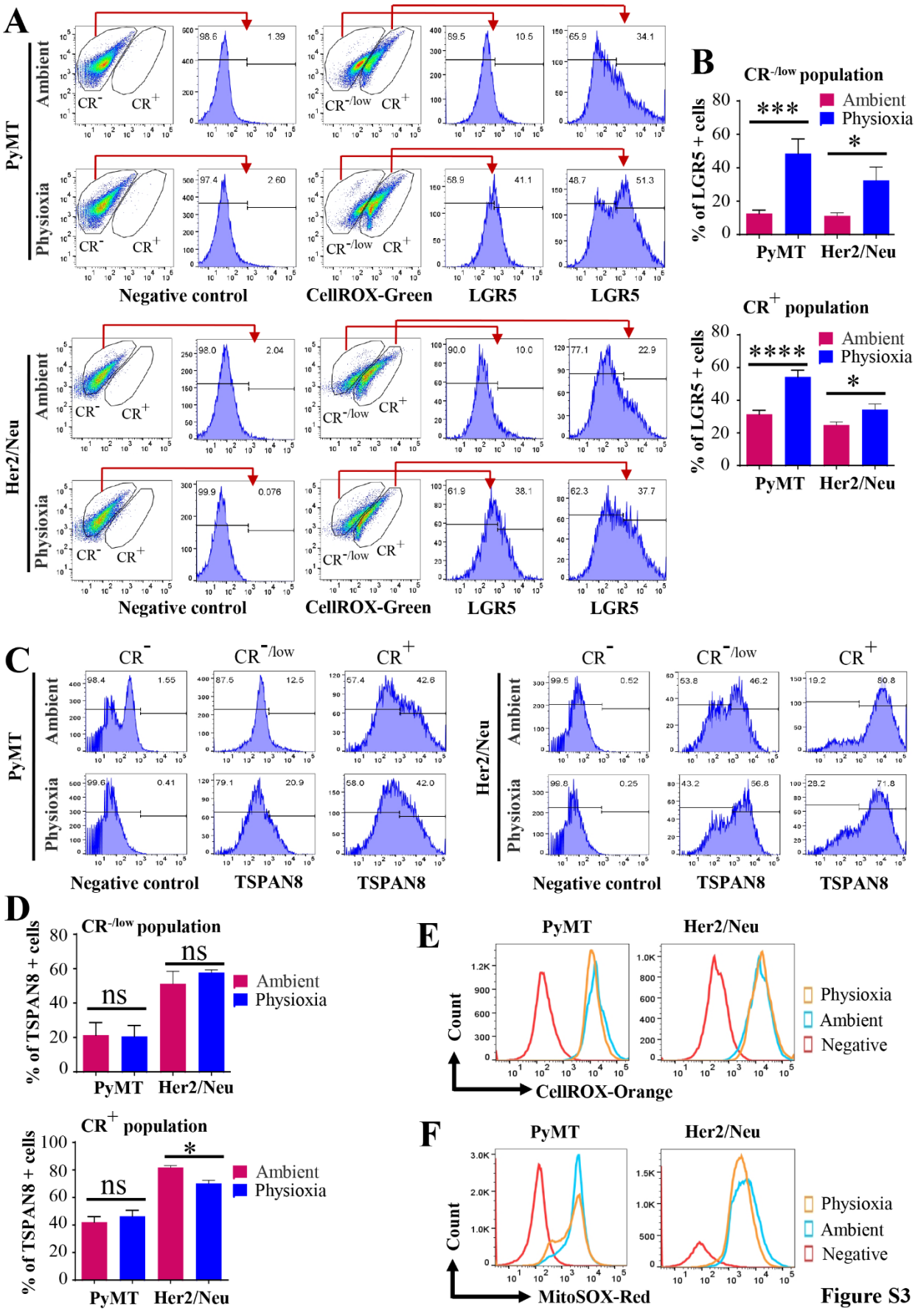
A
PyMT
Her2/Neu
Ambient
Physioxia
CR-
CR+
CR-/low
Negative control
CellROX-Green
LGR5
B
CR-/low population
CR+ population
% of LGR5 + cells
Ambient
Physioxia
PyMT
Her2/Neu
C
TSPAN8
D
% of TSPAN8 + cells
ns
E
Count
CellROX-Orange
Negative
F
MitoSOX-Red

Figure S3

fig. S3: LGR5 positivity of CellROX-Green^{+} populations, representing cells with nuclear ROS, was higher under physioxia compared to ambient air. (A) Representative flow cytometry data showing staining patterns of CellROX-green$^{-/low}$ (CR$^{-/low}$) and CellROX-green^{+} (CR^{+}) populations in PyMT and Her2/Neu tumor cells and enrichment of LGR5^{+} cells in both populations. (B) Quantitation of LGR5^{+} cells in CellROX-green$^{-/low}$ and CellROX-green^{+} populations in PyMT and Her2/Neu tumor cells (n=3-4). (C) Representative flow cytometry data showing TSPAN8^{+} cells in CellROX-green$^{-/low}$ and CellROX-green^{+} populations in PyMT and Her2/Neu tumor cells. (D) Quantitation of TSPAN8^{+} cells in CellROX-green$^{-/low}$ and CellROX-green^{+} populations in PyMT and Her2/Neu tumor cells (n=3-4). (E) Tumor cells collected and processed under physioxia and processed under ambient air were stained with CellROX-orange and subjected to flow cytometry (n=4). (F) Tumor cells collected and processed under physioxia and processed under ambient air were stained with MitoSOX or vehicle control and analyzed by flow cytometry (n=4).

A

PyMT		Her2/Neu	
Ambient	**Physioxia**	**Ambient**	**Physioxia**
Carcinoma	Carcinoma	Carcinoma	Carcinoma
Carcinoma	Undifferentiated squamous cell carcinoma	Undifferentiated squamous cell carcinoma, Lymphoma	Undifferentiated squamous cell carcinoma, Lymphoma
Adeno squamous	Adeno squamous	Anaplastic squamous cell, Lymphoma	Undifferentiated squamous cell carcinoma, Lymphoma
		Undifferentiated squamous cell carcinoma, Lymphoma	Undifferentiated squamous cell carcinoma
		Carcinoma	Lymphoma, Carcinoma
		Lymphoma, Carcinoma	Carcinoma

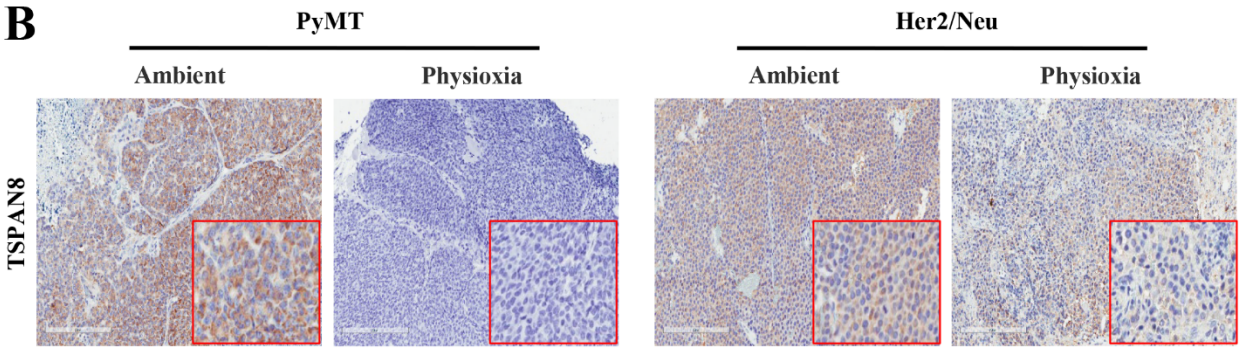

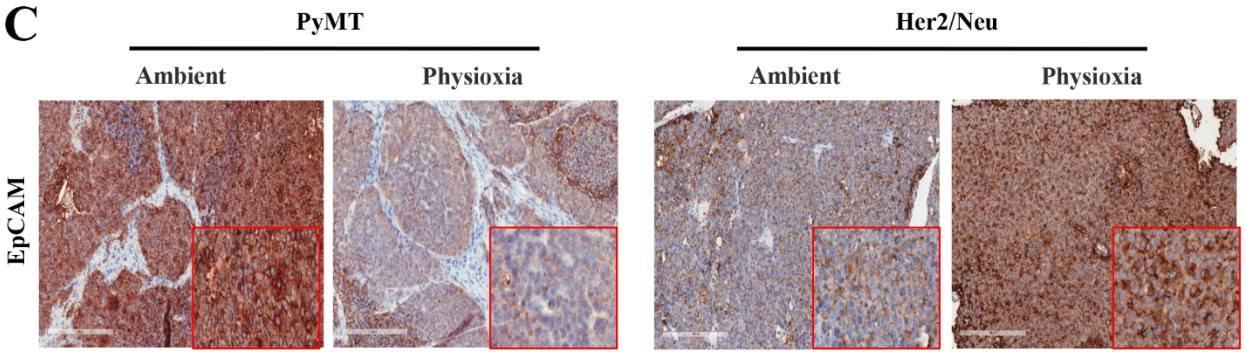

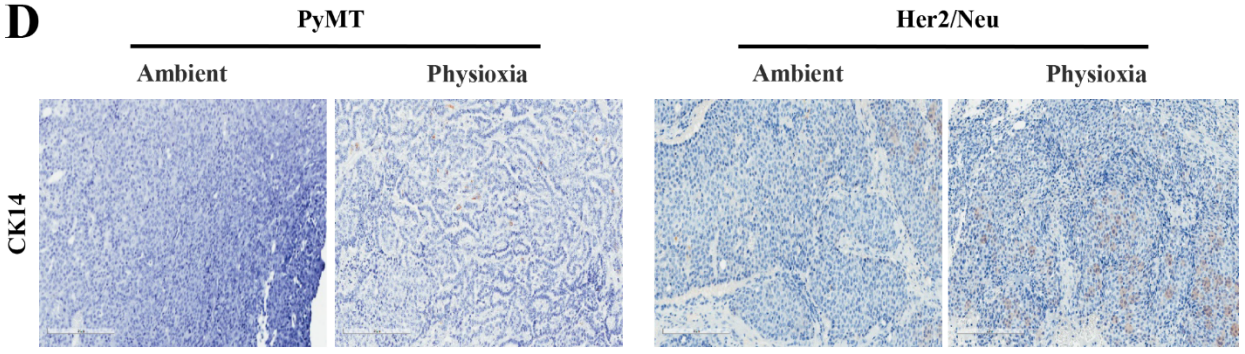

Figure S4

fig. S4: Histology of tumors developed from re-implanted tumor cells collected and processed under physioxia or processed under ambient air. (A) Tumor histotype designated by a pathologist based on H&E staining patterns (n=7). (B) Immunohistochemistry for TSPAN8 (n=7). (C) Immunohistochemistry for EpCAM (n=7). (D) Immunohistochemistry for CK14 (n=7). CK14 negativity suggests that tumors have retained luminal characteristics.

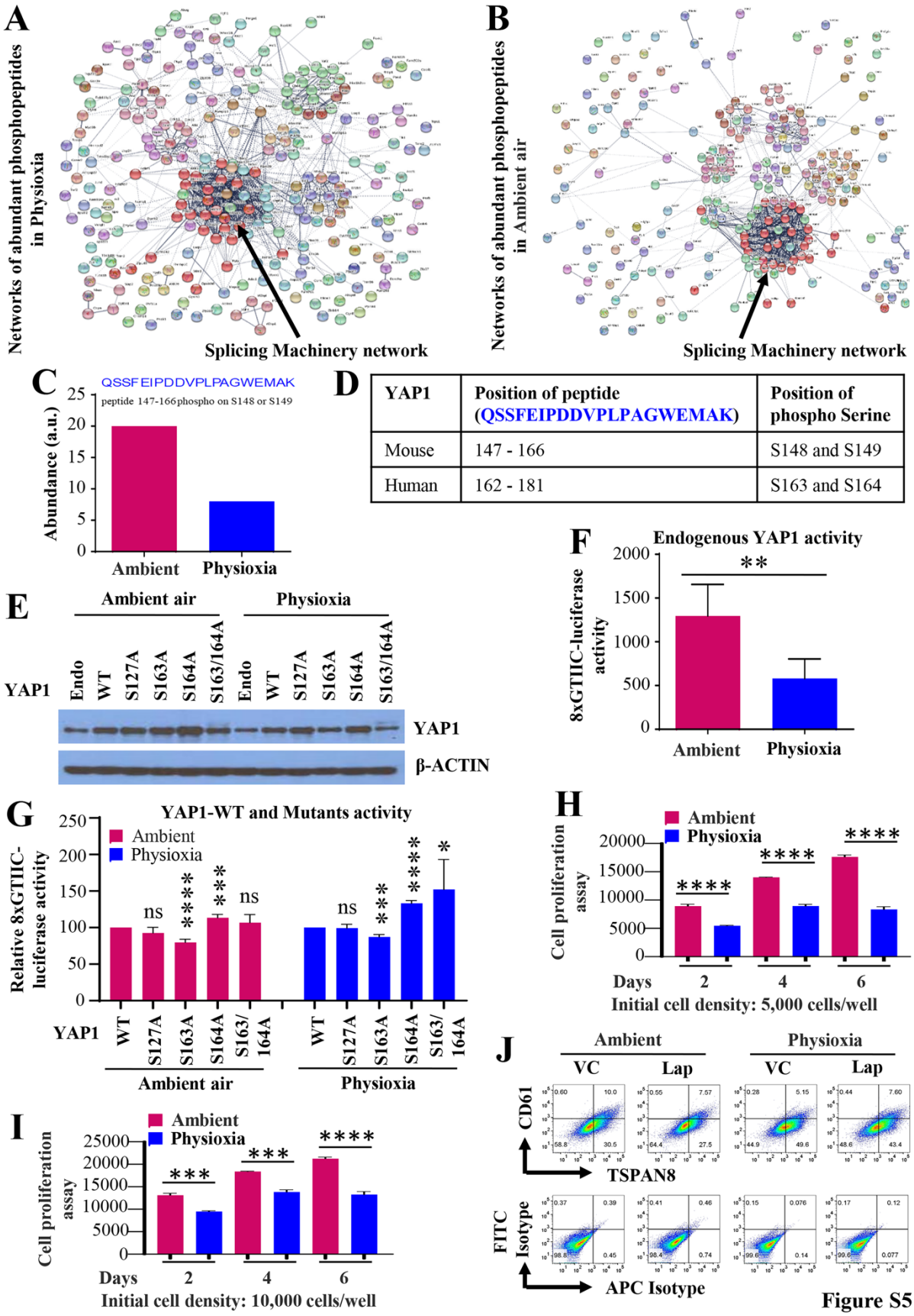

YAP1	Position of peptide (QSSFEIPDDVPLPAGWEMAK)	Position of phospho Serine
Mouse	147 - 166	S148 and S149
Human	162 - 181	S163 and S164

Figure S5

fig. S5: Phospho-proteomics reveal a specific effect of physioxia on splicing machinery and YAP1 signaling. (A) STRING network analysis of phospho-proteins abundant under physioxia. (B) STRING network analysis of phospho-proteins abundant under ambient air. (C) Phosphoproteomics show decreased phosphorylation on either S148 or S149 within the peptide spanning residues 147-166 under physioxia relative to ambient air. (D) Table shows phosphopeptide position in mouse YAP1 and position of the phosphoserines, including corresponding positions in human YAP1. (E) Western blots show expression of YAP1 in HEK293T cells transfected with the indicated plasmid constructs under ambient air and physioxia. HEK293T cells were grown and transfected with indicated plasmid constructs under physioxia, cells were split into two equal parts 24 hours post-transfection, with one portion grown in physioxia and the other in ambient air. Cells were lysed after 24 hours for western blotting. Endo, endogenous expression. (F) Decreased endogenous YAP1 activity under physioxia compared to ambient air as indicated by luciferase reporter activity (n=5). (G) Differential YAP1 activity in HEK293T cells co-transfected with indicated plasmid constructs and 8xGTIIC luciferase under physioxia and ambient air (n=5). Activity of wild type YAP1 was normalized to 100 and relative activity of mutants with specific non-phosphorylatable residues is shown. (H and I) Tumor cells processed and grown under ambient air showed higher proliferation rate. Indicated number of PyMT tumor cells were plated in 96 well plates and cell proliferation rates were measured on indicated days after plating (n=6). (J) CD61/TSPAN8 staining pattern of tumor cells from transplanted PyMT tumor xenografts developed from tumor cells collected and processed under ambient air and physioxia, and treated daily with 100 mg/kg body weight lapatinib (Lap) or vehicle control (VC) via oral gavage for 25 days (n=3). ***$p<0.001$, ****$p<0.0001$ by ANOVA.

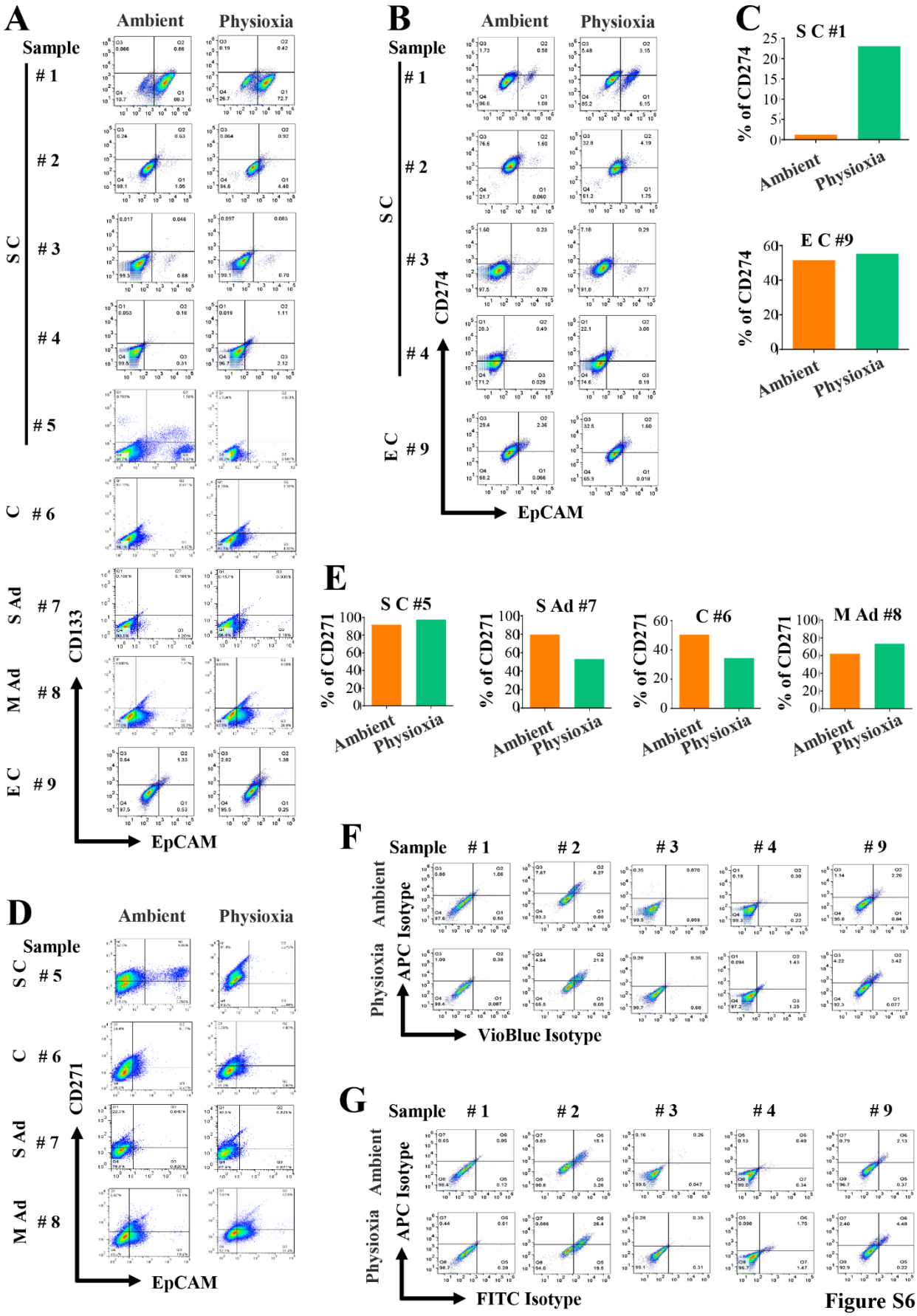
A
Ambient
Physioxia
Sample
1
2
3
4
5
6
7
8
9
S C
C
S Ad
M Ad
E C
CD133
EpCAM
B
Ambient
Physioxia
Sample
CD274
EpCAM
C
S C #1
% of CD274
Ambient
Physioxia
E C #9
D
CD271
E
S C #5
S Ad #7
C #6
M Ad #8
% of CD271
F
Sample
APC Isotype
VioBlue Isotype
G
FITC Isotype

Figure S6

fig. S6: Characterization of cells from ascites fluids collected and processed under physioxia and ambient air. (A) CD133/EpCAM staining pattern of lineage-negative cells from ascites fluid (n=9). (B) CD274/EpCAM staining pattern of cells from ascites fluid (n=5). (C) Cells cultured from ascites fluid of a serous carcinoma under physioxia showed elevated levels of $CD274^{+}$ cells. (D) CD271/EpCAM staining pattern of cells from ascites fluids (n=4). (E) Physioxia displayed tumor subtype-specific effects on $CD271^{+}$ cells. (F and G). Isotype control antibody staining patterns for cells derived from ascites fluids that measured CD49f-APC/EpCAM-VioBlue, CD44-APC/CD24-FITC, CD133-APC/EpCAM-VioBlue, CD274-APC/EpCAM-VioBlue and CD271-APC/EpCAM-VioBlue.

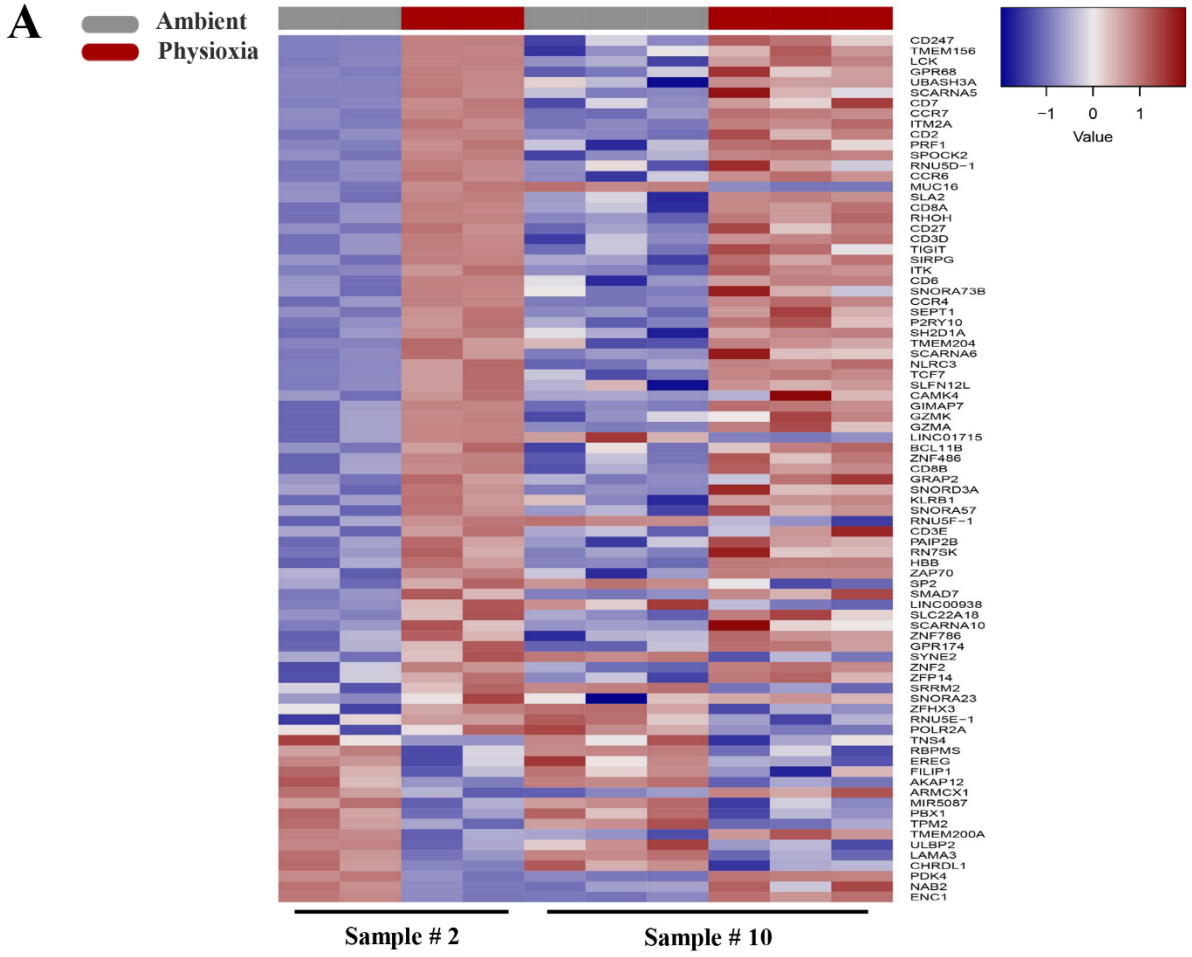

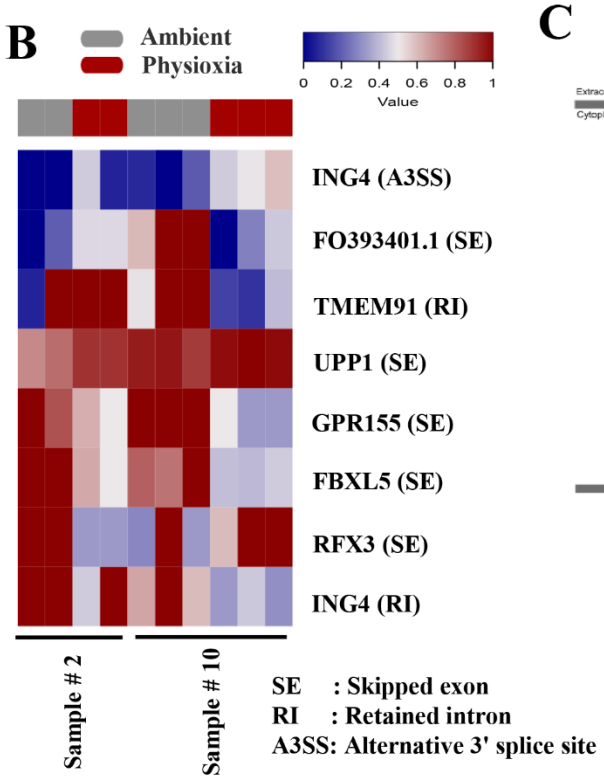

SE : Skipped exon
RI : Retained intron
A3SS: Alternative 3' splice site

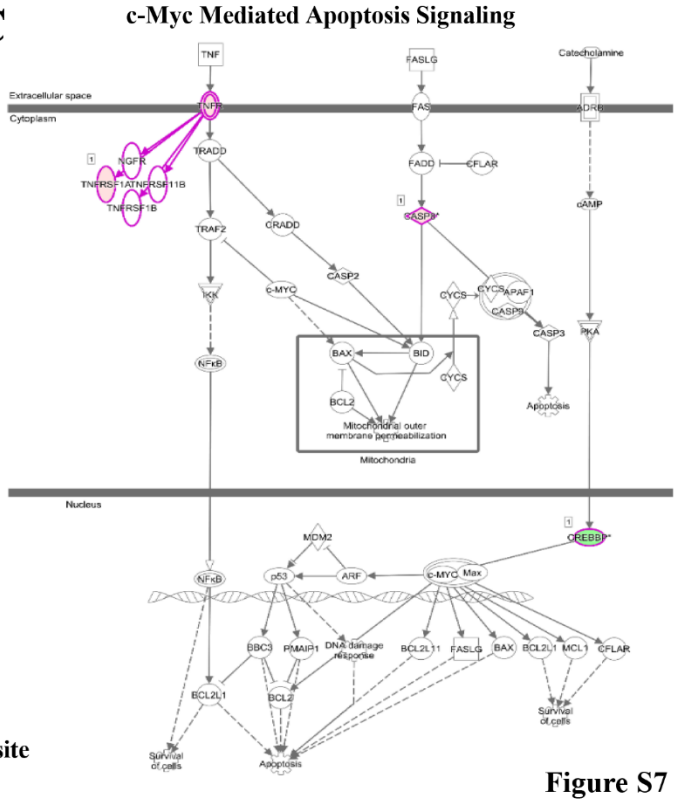

Figure S7

fig. S7: Heatmap of genes differentially expressed and alternatively spliced genes in cells of ascites fluid collected and processed under physioxia compared to that collected and processed under ambient air. (A) Heatmap of differentially expressed genes in cells collected and processed under physioxia compared to cells collected and processed under ambient air. Differentially expressed genes from independent analyses were filtered for FDR <= 0.05 and absolute log2FC >= 0.5. Genes passing filters and common in both patients were then used to generate the heatmap. Log2FPKM values were centered and scaled by gene in each experiment separately. Color bar at the top denotes ambient air or physioxia condition. (B) Heatmap of differentially spliced genes in cells collected and processed under physioxia compared to cells collected and processed under ambient air. Differentially spliced events from all event types were merged and filtered in both experiments. Events having an FDR <= 0.05 and a minimum number of 5 inclusion or exclusion reads across all replicates in a group, as well as having at least 1 inclusion or exclusion read in all replicates from both groups, were kept. These filters ensured events were significant, sufficiently covered and consistently present respectively. Inclusion levels of the remaining 8 exons were directly plotted for each gene and sample replicate. Color bar at the top denotes ambient air (gray) or physioxia (red) condition. (C) Ingenuity pathway analysis (IPA) of alternatively spliced genes under physioxia compared to ambient air. These genes are part of cMyc-mediated apoptotic pathways.